

Kondo effect in carbon nanotubes at half filling

B. Babić, T. Kontos, and C. Schönberger*

Institut für Physik, Universität Basel, Klingelbergstr. 82, CH-4056 Basel, Switzerland

(Received 6 July 2004; published 22 December 2004)

In a single state of a quantum dot the Kondo effect arises due to the spin-degeneracy, which is present if the dot is occupied with one electron ($N=1$). The eigenstates of a carbon nanotube quantum dot possess an additional orbital degeneracy leading to a fourfold shell pattern. This additional degeneracy increases the possibility for the Kondo effect to appear. We revisit the Kondo problem in metallic carbon nanotubes by linear and nonlinear transport measurement in this regime, in which the fourfold pattern is present. We have analyzed the ground state of CNTs, which were grown by chemical vapor deposition, at filling $N=1$, $N=2$, and $N=3$. Of particular interest is the half-filled shell, i.e., $N=2$. In this case, the ground state is either a paired electron state or a state for which the singlet and triplet states are effectively degenerate, allowing in the latter case for the appearance of the Kondo effect. We deduce numbers for the effective mismatch δ of the levels from perfect degeneracy and the exchange energy J . While $\delta \sim 0.1-0.2$ (in units of level spacing) is in agreement with previous work, the exchange term is found to be surprisingly small: $J \lesssim 0.02$. In addition we report on the observation of gaps, which in one case is seen at $N=3$ and in another is present over an extended sequence of levels.

DOI: 10.1103/PhysRevB.70.235419

PACS number(s): 73.63.Fg, 73.63.Kv, 73.23.Hk, 72.15.Qm

I. INTRODUCTION

In the past decade, transport measurements have emerged as a primary tool for exploring the electrical properties of structures on the nanometer scale. Due to their unique electronic bandstructure, much attention has been focused on carbon nanotubes (CNTs).¹ For metallic single wall carbon nanotubes (SWNTs) just two spin degenerate one-dimensional ($1d$) modes should govern their transport properties at low energies, which makes them interesting model systems to explore the physics in reduced dimensions.²

Due to the finite length, given by the lithographically fabricated contacts on opposite sides of the CNT (two-terminal device with source and drain contacts), the one-dimensional CNT is turned into a quantum dot³ at low temperatures (typically at $\lesssim 10$ K), i.e., into a zero-dimensional object with a discrete level spectrum. The confinement is formed by the finite back-reflection at the edges of the contacts. The level spacing δE is determined by the contact separation L and is inversely proportional to it. This picture in the box-model holds provided the level-broadening Γ and the temperature are both smaller than δE . Γ describes the life-time broadening proportional to the coupling strength to the leads.

Until now, three transport regimes have been identified in SWNTs: A) single-electron tunneling,⁴ which is dominated by the on-site Coulomb repulsion expressed by the energy term $U=e^2/C_\Sigma$, where C_Σ is the total capacitance; B) the regime of correlated transport, in which higher-order tunneling processes, are appreciable, leading to the emergence of the Kondo effect;^{5,6} and C) the open SWNT for which Coulomb interaction may be neglected and the residual gate-dependence of G can be described as in a tunable Fabry–Perot resonator.⁷ A) holds for low, B) for intermediate and C) for high transparent contacts. The Kondo effect, which occurs at intermediate contact transparency, can be seen as the Holy Grail of many electron physics. It has first been ob-

served in quantum dots by Goldhaber-Gordon *et al.*⁵ and in CNTs by Nygård *et al.*⁸ In contrast to the Coulomb blockade (CB) regime, which only probes the electrons confined on a QD, the Kondo effect incorporates delocalized electrons in the leads coherently. The presence of a degenerate ground state in the quantum dot (for example, a singly occupied level with twofold degeneracy due to the spin degree of freedom) forms the basis for the Kondo effect. A multitude of coherent second- and higher-order elastic tunneling processes between the Fermi seas of the leads and the quantum-dot state are enabled, leading to the appearance of a narrow peak in the density of states (DOS) right at the Fermi level (the Kondo resonance) at sufficiently low temperatures. Its width is given by the Kondo temperature T_K which measures the binding energy of this many-electron state. The peak in the DOS enhances the probability for electrons to tunnel from source to drain. As a consequence the zero-temperature linear-conductance saturates at the quantized conductance $G_0=2e^2/h$ (unitary limit), provided the device is coupled symmetrically to source and drain.

As in atoms, eigenstates in quantum dots (QDs) may be degenerate due to symmetries and together with the spin degeneracy and Pauli principle lead to the formation of electronic shells. Indeed, striking shell patterns have been observed in QDs.^{9,10} The eigenstates (Bloch-states) at the Fermi energy of graphene (two-dimensional sheet of graphite) is twofold degenerate. The two wave functions correspond to the two carbon sublattices (the unit-cell is composed of two C-atoms). This degeneracy is preserved in CNTs and should therefore lead to two degenerate orbitals in a finite-length nanotube in $0d$. Together with the spin degeneracy, the shells are expected to be fourfold degenerate. This shell pattern has recently been observed by Buitelaar and co-workers¹¹ in multi-wall carbon nanotubes (MWNTs) and by Liang *et al.* in SWNTs.¹³ Within one shell the ground-state spin was shown to follow the sequence $S=0 \rightarrow \frac{1}{2} \rightarrow 0 \rightarrow \frac{1}{2}$ in the

former work, whereas a possible triplet ground state for two added electrons was suggested by the latter authors, i.e., the sequence $S=0 \rightarrow \frac{1}{2} \rightarrow 1 \rightarrow \frac{1}{2}$.

Here we focus on CVD-grown metallic carbon nanotubes (CNTs).^{12,14} We will first examine the fourfold shell pattern in great detail and demonstrate that the half-filled ground state (i.e., two electrons added to an empty shell) is either a paired electron with $S=0$ or the six possible two-electron states are effectively degenerate due to a level broadening exceeding the orbital mismatch and exchange energy. We furthermore have discovered striking gaps in several samples. This anomaly is at present not understood.

II. EXPERIMENTAL

Single wall carbon nanotubes (SWNTs) have been grown from patterned catalyst islands by the chemical vapor deposition method on Si/SiO₂ substrates.¹⁵ The degenerately doped silicon, terminated by a 400 nm thick SiO₂ layer, is used as a back-gate to modulate the electrochemical potential of the SWNT electrically contacted with a source and drain terminal. The contacts are patterned by electron-beam lithography (EBL) using polymethylmethacrylate (PMMA) as resist, followed by metallization with palladium and lift-off.^{14,16} Once the samples are made, semiconducting and metallic SWNTs are distinguished by the dependence of their electrical conductance G on the gate voltage V_g measured at room temperature ($T \approx 300$ K).¹⁴ In the rest of the paper we report on measurements performed on metallic SWNTs with relatively low-ohmic contacts, such that co-tunneling and Kondo physics is observable.

The electrical characterization of the devices has been performed at low temperature in a ³He system at 300 mK. We measure the electrical current I with a low noise current to voltage amplifier as a function of source-drain (V_{sd}) and gate (V_g) voltage and determine the differential conductance $G_d := \partial I / \partial V_{sd}$ numerically. Finally, the collected data $G_d(V_{sd}, V_g)$ are represented in a two-dimensional gray-scale representation in which the gray-scale corresponds to the magnitude of G_d . The linear-response conductance $G := I / V_{sd}$ with $V_{sd} \rightarrow 0$ is measured at a small but finite source-drain voltage of 40 μ V.

III. RESULTS AND DISCUSSION

In this section, we will focus first on one set of measurements which we will analyze in great detail. This set of data is shown in Fig. 1. Figure 1(a) shows the linear-response conductance G as a function of gate voltage V_g . Figures 1(b) and 1(c) display the corresponding gray-scale plots of the differential conductance G_d in zero magnetic field and $B = 5$ T, respectively. White corresponds to low and black to high conductance.

The observed patterns correspond to a quantum dot with a relatively strong coupling to the contacts. Signatures of the latter are high conductance “ridges,” observed at zero bias ($V_{sd} \approx 0$) and $B=0$, caused by the the Kondo effect. This effect is a many-electron effect and requires a relatively high tunneling coupling to the leads in order to be appreciable at

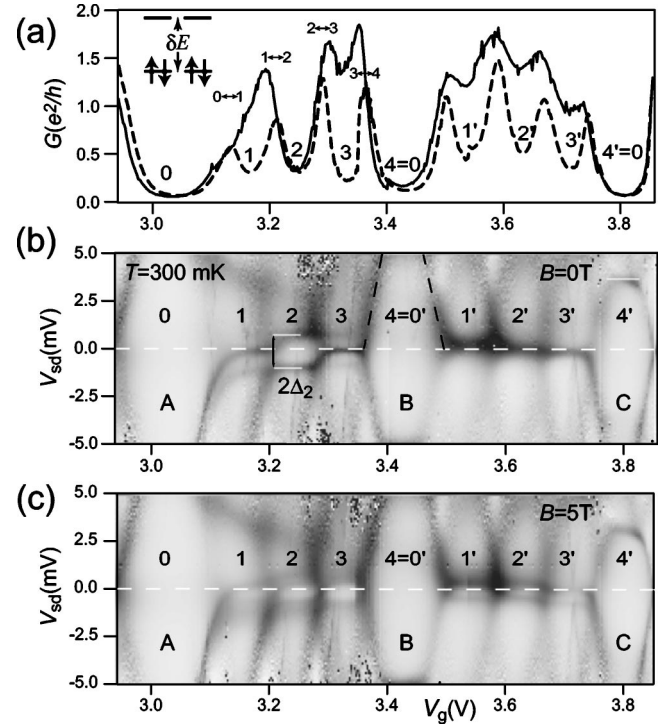


FIG. 1. (a) Linear response conductance G as a function of back-gate voltage V_g of a SWNT device with contact separation $L \sim 300$ nm (edge-to-edge of reservoirs), measured at $T=300$ mK and in a magnetic field of $B=0$ (solid curve) and $B=5$ T (dashed curve). A clear clustering in four peaks is observed (pronounced in magnetic field), which suggests a single-electron shell pattern with fourfold degeneracy. Charge states corresponding to a filled shell (inset) are labelled as 0 or 4. (b,c) Corresponding gray-scale plots of the differential conductance dI/dV_{sd} (darker more conductive) at $B=0$ (b) and $B=5$ T (c) as a function of gate V_g and source-drain voltage V_{sd} . In the first shell, high conductance Kondo ridges (visible at $V_{sd} \sim 0$) are observed for charge states 1 and 3, whereas they appear for states 1', 2', and 3' in the second shell. The Kondo ridges clearly split in the applied magnetic field.

temperatures where the measurements take place. As required,^{5,6} we find that G increases if the temperature is lowered below ≈ 4 K to saturate at the lowest temperature close to the unitary limit of $G=2e^2/h$. The characteristic energy scale, i.e., the Kondo temperature T_K , has been deduced from the temperature dependence of G in ridge 3 (not shown) and found to be $T_K \approx 2$ K. The conductance enhancement due to the Kondo effect is observed at zero source-drain voltage if $B=0$. In a magnetic field, however, the conductance enhancement is reduced and a splitting of the peak conductance to finite source-drain voltages is expected.^{5,17} This splitting is visible in Fig. 1(c) which was measured in a perpendicular magnetic field of 5 T. That the linear-response conductance G is suppressed in a magnetic field is clearly seen in Fig. 1(a) in which the solid (dashed) curve corresponds to $B=0$ ($B=5$ T).

Because the many-electron effects (Kondo effect) are suppressed in a magnetic field, we can use the linear-response conductance measurement in a magnetic field [dashed curve in Fig. 1(a)] to assign the charge states of the quantum dot with reference to the single-electron tunneling picture. A

transition from a ground state with N electrons in the dot to one with $N+1$ gives rise to a peak in the conductance, whereas G is suppressed in between. This pattern is nicely seen in the dashed curve of Fig. 1(a), in which transitions have been labelled. Evidently, these conductance peaks form a repeating pattern in clusters of four. This pattern is the generic shell pattern of an ideal CNT quantum dot.^{11,13} It is caused by the fourfold degeneracy of $0d$ -eigenstates, two of which stem from spin and the other two from the so-called $K-K'$ orbital-degeneracy of graphene.¹ The fourfold pattern can be regarded as a measure of the quality of the SWNTs. It is not observed in all SWNTs and, even if observed, it is not usually present over the whole gate voltage range. But it can repeat over several shells, not just two as shown in Fig. 1. The degeneracy may be lifted by disorder and by the contacts which may couple differently to the two orbital states. As has been pointed out by Oreg *et al.*, the fourfold pattern may be absent even in a “perfect” SWNT because the two orbital states can respond differently to the electrostatic gate-field if inhomogeneous.¹⁸

Let us continue to analyze our data in terms of the constant-interaction model.¹⁹ In order to assign the states only two parameters are needed: the single-electron charging energy $U := e^2/C_\Sigma$ (which can be expressed by the total capacitance C_Σ and is assumed to be a constant in this model) and the single-electron level spacing δE . Note, that δE measures the energy difference between a filled shell to a state with one additional electron. This is sketched in the inset of Fig. 1(a). To add an electron one has to provide an “addition energy” composed of charging energy U plus level-spacing δE , the latter only if the electron must be added into a new shell. Therefore, the addition energy ΔE equals $\delta E + U$ for the first electron in a shell, whereas it amounts to “only” U for the following three added electrons belonging to the same shell. Since ΔE is proportional to the gate-voltage difference between adjacent conductance peaks (the conversion factor equals eC_g/C_Σ), the labelling of states in terms of charge N in Fig. 1(a) should be understandable. $N=0 \bmod 4$ corresponds to a ground state with a filled shell. Due to the large addition energy, the conductance is strongly suppressed for a filled shell, giving rise to the diamond like white areas (denoted by A, B and C) in the gray-scale plots. Adding electrons to the filled shell one by one [peaks in G , dashed curve of Fig. 1(a)], we reach the state $N=4$ which corresponds again to a filled shell.

In the following, the ground states will be labelled by $N=0, \dots, 3$ for the first quartet and $N=0', \dots, 3'$ for the second, where $N=4=0'$. Relying on the constant interaction model, the ratio between the average level spacing and charging energy amounts to $\delta E/U \approx 1$ in our data. It is seen, however, that U is constant to a good approximation, but that δE varies. For the respective diamonds A, B and C, the level spacing δE amounts to $\approx 7, 5$, and 3 meV, respectively. Theoretically, the level spacing of an ideal SWNT is given by $\delta E = \hbar v_F/2L$, where $v_F = 8 \times 10^5$ m/s is the Fermi velocity and L the length of the tube that determines the $1d$ cavity.¹ Taking the nanotube length L measured from the edges of the contacts, which for this sample amounts to $L \sim 300$ nm, the equation predicts a level spacing of $\delta E \sim 5.5$ meV in good agreement with the experimental values of $3-7$ meV. The

data in Fig. 1 yields for the charging energy $U = 5.3 \pm 0.5$ meV and a gate-conversion factor of $\alpha := C_g/C_\Sigma$ of 0.08.

Focusing on the high-conductance Kondo ridges at zero bias voltage, we see in Fig. 1(b) a ridge at charge states $N=1$ and $N=3$, whereas G is suppressed at half-filling, i.e., at $N=2$. The situation is different for the second quartet, where Kondo ridges are observed for all three states $N=1, 2$ and 3 . This phenomenon was reported before by Liang *et al.*¹³ Whereas a spin- $\frac{1}{2}$ Kondo effect is expected for $N=1$ (one electron) and $N=3$ (one hole), the situation at half-filling, i.e., at $N=2$, is less obvious. The observed Kondo effect was assigned to a spin-1 triplet state in Ref. 13. In the following we reexamine this assignment. To do so, we have to go beyond the “free” electron model and consider among other things the exchange interaction. There are three additional parameters: First, it has been pointed out that the orbital degeneracy need not be exact.^{11,13} The orbital mismatch is denoted by δ . With regard to on-site charging energy the double occupancy of one orbital is a bit higher in energy as compared to placing each of the two electrons in a separate orbital. This parameter has been introduced by Oreg *et al.*¹⁸ and is denoted by δU . Finally, placing the two electrons in different orbitals gives rise to a spin-dependent exchange energy term, which according to Hund’s rule favors the triplet state, i.e., the state with spin $S=1$. This parameter is denoted by J . These parameters have been extracted, both for MWNTs¹¹ and SWNTs,¹³ and the analysis of our data confirms the previously obtained values. The importance of the parameters in descending order is δ, J and δU as the least important one. The former work by Buitelaar *et al.* reports $\delta \approx 0.2$ and $J < 0.09$ and the latter work by Liang *et al.* reports $\delta \approx 0.3, J \approx 0.1$ and $\delta U < 0.1$ (all numbers are measured in units of level spacing δE). We neglect δU because it is small and typically much smaller than the bare level broadening Γ , which—as we will emphasize—matters as well. Since the Kondo effect is the dynamic screening of the local spin by exchange with a sea of electrons, it is tempting to assign the Kondo ridge for $N=2$ to a spin-1 (triplet) ground state. However, with regard to the just mentioned parameters, this appears to be unlikely, because $J < \delta$, favoring a spin-0 ground state.¹⁸

Let us first contrast the possible states at $N=1$ and $N=2$ for the case of degenerate orbitals ($\delta=0$) and without exchange ($J=0$), shown in Fig. 2(a), with the case of a finite level mismatch and a finite exchange energy, shown in Fig. 2(b). In the first (maybe too naive) model of Fig. 2(a), the degeneracy equals 4 at $N=1$ and clearly Kondo physics can emerge. At $N=2$ the degeneracy is even larger, amounting to 6 and second-order elastic spin-flip processes are energetically allowed so that Kondo physics can emerge as well. Here, two states are paired-electron states and the other four may be labelled as one singlet state with spin $S=0$ and three triplet states with $S=1$, denoted as S and T states. The Kondo effect may be expected to be even enhanced in this case due to the larger number of states.²⁰ This scenario corresponds to the Kondo effect for which the singlet and triplet states are degenerate. This has been realized experimentally in semiconducting quantum dots by tuning the states with either a magnetic or an electric field.²⁰⁻²² Once we go over to the

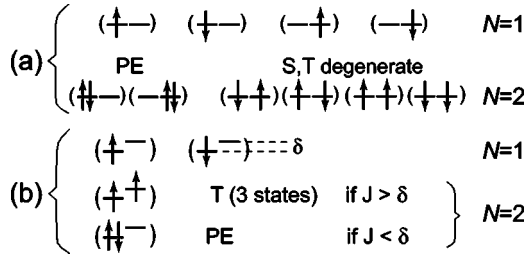


FIG. 2. Illustration of the state-filling scheme for one ($N=1$) and two ($N=2$) excess electrons. In (a) the level-mismatch δ and the exchange energy J are zero, whereas these parameters are nonzero in (b). PE denotes a paired-electron state, and S (T) denotes the singlet (triplet) two electron state. The Kondo effect may arise in three cases: obviously for the spin- $\frac{1}{2}$ with one excess electron ($N=1$) and if $N=2$ for the spin-1 triplet state, but also for the case for which $\delta=J=0$, i.e., when the singlet and triplet states are degenerate (ST state).

more realistic model shown in Fig. 2(b), assuming that exchange and level mismatch are nonzero and of comparable magnitude, the $N=1$ states remains “normal” in the sense that only the lowest lying orbital need to be considered. At half-filling, i.e., at $N=2$, there are however two possibilities:¹⁸ if exchange dominates ($J > \delta$), the ground state is the spin triplet (T) state, whereas if the opposite holds, the ground state is a paired electron (PE) residing on the lowest orbital state. The energy difference between the T and PE states is given by $\Delta = \delta - J$.²³ Although the Kondo effect is (in principle) possible for the triplet, there is no Kondo effect possible for paired electrons. Note that, unlike previous discussions, there are *three* cases to consider at half-filling. Two may give rise to Kondo and one does not. To have an abbreviation at hand we denote the three $N=2$ states with ST (degenerate ground state), PE (paired electron ground state) and T (triplet ground state). As mentioned above, the Kondo ridge at $N=2$ has been assigned to the triplet state.¹³ Though this is tempting at first sight, there is no necessity. In fact, this assignment is unlikely, first because J is measured to be small (usually smaller than δ) and, second, the Kondo temperature T_K for triplet Kondo is predicted to be much smaller than T_K for $S = \frac{1}{2}$ -Kondo²⁴ (an estimate will follow below).

We now look at the excitation spectra for $N=1, 3$ and $N=2$ in zero field. This is shown in Figs. 3(a)–3(c), where (a) and (b) correspond to odd filling ($N=1, 3$) and (c) to half-filling ($N=2$). The energy Δ of the first excited state at fixed N relative to the ground state is given by the level mismatch δ , both for $N=1$ and $N=3$, i.e., $\Delta_{1,3} = \delta$. This is illustrated in the respective insets on the right. The first excited states show up as a conductance peak at finite V_{sd} , corresponding to the excitation energy. This is a so-called inelastic co-tunneling process. We obtain from the measurement $\Delta_1 = 0.92$ meV and $\Delta_3 = 0.85$ meV. Hence, the level mismatch is given by 0.89 ± 0.4 meV. For the $N=2$ case we have to distinguish two possibilities: if $J > \delta$, the ground state is the triplet (T) and the excited state the paired electron (PE) state, yielding $\Delta_2 = J - \delta$. If, on the other hand, $J < \delta$, the states are reversed, yielding $\Delta_2 = \delta - J$. In general, $\Delta_2 = |\delta - J|$. From the experiment [Fig. 1(c)] we deduce $\Delta_2 = 0.88$ meV. We stress

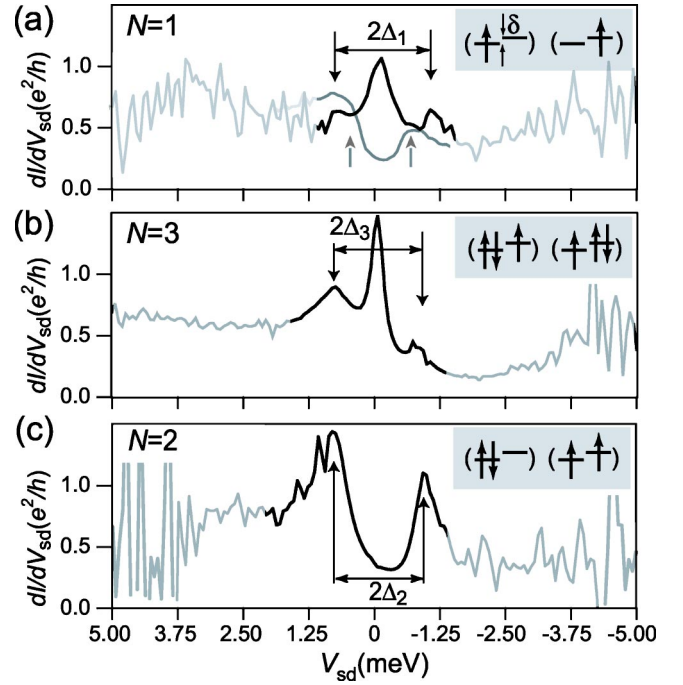


FIG. 3. Nonlinear differential conductance dI/dV_{sd} as a function of V_{sd} at $V_g = \text{const}$ deduced from the data shown in Fig. 1(b) at zero magnetic field. (a) and (b) correspond to the states $N=1$ and $N=3$, whereas (c) corresponds to the half-filled shell $N=2$. All three dI/dV_{sd} cuts have been placed in the middle of the charge state. The visible excitation peaks occur at energy Δ and are due to inelastic co-tunneling through the excited state. The relevant states are illustrated in the respective insets on the right. The gray curve in (a) has been measured in a magnetic field of 5 T. Arrows point to $\Delta_Z = g\mu_B B = 0.58$ meV using $g=2$.

that we measure on one and the same shell so that we can use the parameter δ , measured for the $N=1, 3$ case, also for the $N=2$ case. Comparing the numbers leaves open two possibilities: either the exchange parameter is quite small, i.e., $J \sim 0$ (taking the possible errors into account $J \leq 0.1$ meV), or it is quite large, $J \geq 1.65$ meV. If the latter would be true, it would be a remarkable coincidence that we find $|\delta - J| \sim \delta$ with $J \approx 2\delta$. Moreover, the ratio $J/\delta E > 0.3$ would be quite remarkable with regard to previous measurements. On the other hand, comparable values for J have theoretically been predicted, however only for small diameter tubes. For example, $J/\delta E$ was estimated to be ≥ 0.22 and ≥ 0.44 for (10, 10) and (5, 5) tubes, respectively.¹⁸ However, the diameter d of CVD-grown NTs is known to vary substantial and in particular we find that $d \gtrsim 2$ nm,¹⁴ from which one would theoretically predict an exchange parameter of order $J/\delta E \sim 0.1$, which disagrees with the finding above. If J were indeed as large as 2δ , and therefore $J > \delta$, the triplet state would be the ground state at half-filling, i.e., at $N=2$ and $N=2'$. The Kondo effect at half-filling must then be assigned to the $S = 1$ Kondo effect. To explain the absence of the Kondo effect for $N=2$ and its presence for $N=2'$, one would have to argue that the Kondo temperature is smaller than 300 mK at $N=2$, whereas it is larger at $N=2'$. Pustilnik *et al.*²⁵ showed that the Kondo temperature $T_K^{S=1}$ for the triplet state is smaller than $T_{K,1/2}$ for the spin- $\frac{1}{2}$ case. More precisely, $T_{K,1}$ can be

estimated according to $k_B T_{K,1} = (k_B T_{K,1/2})^2 / \delta E$. The average width of the zero-bias resonances at $N=1, 3$ in the left quartet is measured to be 0.35 meV, yielding as a prediction $T_{K,1} \approx 0.25$ K. In the right quartet the same procedure yields for $N=1', 3'$ a mean width of 0.8 meV, from which one predicts $T_{K,1} \approx 1.5$ K. Hence, the comparison with the measuring temperature does not exclude $S=1$ Kondo, as $T_{K,1} \leq 0.3$ K in the left quartet and $T_{K,1} > 0.3$ K in the right one. However, the ratio $T_{K,1}/T_{K,1/2}$ measured in the right quartet is inconsistent with theory which predicts $T_{K,1/2}/\delta E$. The former is evaluated to 0.8, ..., 1.6, whereas the latter is at most 0.3. In simple terms, the appearance of the two resonances at $N=1'$ and $N=2'$, with essentially one and the same width (1.1 and 0.9 meV, respectively), makes triplet-Kondo quite unlikely.

In magnetic field the states further split due to the Zeeman energy given by $\pm g\mu_B B/2$, where μ_B is the Bohr magneton and g is the so-called g -factor. g has been measured in related electrical measurements on carbon nanotube quantum dots and found to agree with the free electron value of $g=2$.^{3,11,26} Due to the Zeeman splitting the excitation spectrum changes. At $N=1$ and for small magnetic fields (with regard to the level mismatch), the spin- $\frac{1}{2}$ Kondo resonance is expected to split,¹¹ evolving into inelastic co-tunneling with an excitation energy given by $\Delta_Z = g\mu_B B$. Because of the relatively large width of the zero-bias resonances, this shift is hardly visible for small magnetic fields in the experiment. That is why we have chosen a relatively large field of 5 T. This field yields for the Zeeman excitation energy 0.58 meV, taking $g=2$. Note, however, that there is a second excited state given by the level mismatch $\delta \approx 0.9$ meV. If we analyze the nonlinear differential conductance as a function of V_{sd} , we see two excitation lines (one at positive and one at negative bias), which are markedly broadened, suggesting an overlap of two excitation features [see Fig. 3(a) (gray overlaid graph)]. The onset of the excitation peaks agrees with the Zeeman energy (arrows from below). This analysis is of particular importance in the $N=2$ case, because it allows us to distinguish the PE from the T ground state unambiguously (see Fig. 4). If the ground state is the paired-electron state, the first excitation occurs at energy $\Delta_2 = \delta - \Delta_Z - J \approx \delta - \Delta_Z$ (because $J \approx 0$) and the second lies at δ . In contrast, if the ground state is the spin-1 triplet state, the first two excited states have energy $\Delta = J + \Delta_Z - \delta \approx \delta + \Delta_Z$ and $J + \Delta_Z \approx 2\delta + \Delta_Z$ (because $J \approx 2\delta$ in this case). This is shown (approximately to scale) in the illustrations of Figs. 4(b) and 4(c), respectively. Based on the field dependence of the excitation spectrum we can predict the position of the excitation peaks for the two cases. In the measurement, shown in Fig. 4(a), the upper black arrows point to expected excitations if the ground state is the paired-electron (PE) state, whereas the upwards pointing open arrows correspond to the expected excitations for the triplet (T) ground state. It is obvious that the agreement with the PE state is much better. The excitation peaks at zero field do not move out to larger energies expected for the T ground state, but rather shrink. In particular there are clear low-energy shoulders visible which agree quite reasonably with the expected lowest energy excitation energy for the PE ground state.

Taking all arguments together, this makes a convincing case for the ground state at half-filling, i.e., for $N=2$, which

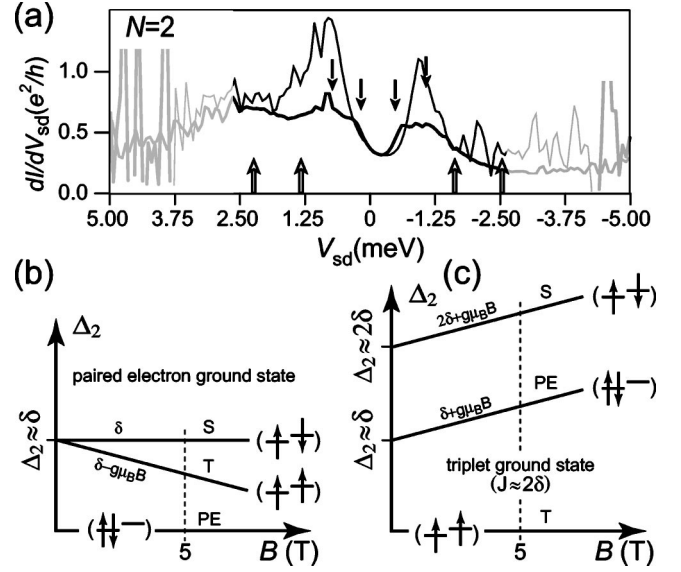


FIG. 4. (a) Nonlinear differential conductance dI/dV_{sd} as a function of V_{sd} taken from the data shown in Fig. 1(b) at a fixed gate-voltage corresponding to $N=2$. The thick (thin) curve was measured in a magnetic field of $B=5$ T ($B=0$ T). (b) and (c) illustrate the magnetic-field dependence of the first two excited states at $N=2$. The two cases are drawn approximately to scale using the fact that J is either ≈ 0 (PE ground state) or $\approx 2\delta$ (T ground state) deduced from the data of Figs. 1 and 3.

is the paired-electron state. Moreover, the exchange energy must be very small. How do we then have to explain the pronounced Kondo ridge at $N=2'$, visible in Fig. 1(b)? As we have pointed out when discussing Fig. 2, there are two cases at half-filling that allow for Kondo: spin-1 Kondo in the case of the triplet state or the degenerate ground state, i.e., the ST state. Based on our previous discussion the former can be excluded, so that the only remaining possibility requires degenerate orbitals. We know that the orbitals are not exactly degenerate. The level mismatch, as deduced from the $N=1-3$ states, amounts to $\delta \approx 0.9$ meV, which is quite appreciable. Due to the relative large width of the zero-bias conductance peaks at $N=1', \dots, 3'$ we are not able to deduce the level mismatch on the second shell along the same lines as before for the first shell. Though it is possible that δ is smaller in the second shell, it is unlikely zero. We emphasize, however, that it is crucial to compare the level mismatch with the level width, due to the tunneling couplings Γ_s and Γ_d to the respective contacts. If $\delta < \Gamma$, where $\Gamma := \Gamma_s + \Gamma_d$, the two orbital states cannot be distinguished and are in effect degenerate. We know from other measurements on carbon nanotubes that Γ may vary a lot with gate voltage. Our picture of the half-filled state is correct, if we can show that Γ is smaller than δ within the first shell, but larger within the second. There are several ways to deduce Γ . One possibility is to deduce it from the width of the excitation features at fixed N , another one is to analyze the transitions at finite bias at the edge of the Coulomb-blockade (CB) diamonds. For the left shell the excitation spectra for states $N=2$ and $N=3$ (see Fig. 3) yield $\Gamma \approx 0.7$ meV, whereas a cut at $V_g = 3.1$ V, corresponding to the transition $0 \leftrightarrow 1$, yields $\Gamma \approx 0.9$ meV. Be-

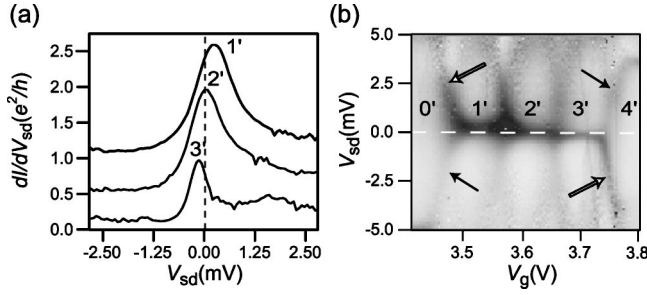


FIG. 5. The Kondo resonance is observed to be offset with respect to the bias voltage V_{sd} for the mixed-valence state with filling $\frac{1}{4}(N=1')$ and $\frac{3}{4}(N=3')$, whereas it is centered at $V_{sd}=0$ at half-filling. (a) shows the respective differential conductance at constant gate voltage corresponding to part (b), which reproduces the second shell of Fig. 1(b). Arrows emphasize an additional asymmetry, discussed in the text.

cause we cannot resolve excitation features in the right shell, we have to rely on transitions at the edge of CB diamonds. We deduce $\Gamma \approx 3$ meV at $0' \leftrightarrow 1'$ and $\Gamma \approx 1.9$ meV at $3' \leftrightarrow 4'$. Clearly $\Gamma \lesssim \delta$ for the left shell and $\Gamma > \delta$ for the right one in support of our statement. To conclude this part, we can say that the Kondo effect at $N=2'$ is not a triplet Kondo, but arises because Γ is larger than the level mismatch, resulting in a ground state in which the paired-electron, the singlet and triplet states are effectively degenerate. Our data is only consistent with a very small exchange term of $J/\delta E \lesssim 0.02$. Such a small value can only be reconciled with theory¹⁸ if either the tube has a large diameter of order ~ 10 nm or the interaction is locally screened, possibly by the presence of other nanotubes forming a bundle.

Examination of the measured data shows that for the Kondo resonances labelled with $1'$ and $3'$ in Fig. 1(b), the positions of the maximum conductance are situated at non-zero bias. This is shown in Fig. 5. This phenomenon has been observed in semiconducting quantum dots and was termed the anomalous Kondo effect by Simmel *et al.*²⁷ It was suggested by these authors that the effect is due to asymmetric and energy-dependent coupling strengths Γ_s and Γ_d to the two reservoirs. The effect has thereafter been confirmed theoretically in a single-impurity Anderson model.²⁸ The authors show that the peak conductance is shifted provided that $\Gamma_s \neq \Gamma_d$, but an energy dependence of $\Gamma_{s,d}$ is not required. We stress here, however, that the Anderson model introduces an additional model-dependent asymmetry in that $U \rightarrow \infty$, which is not realized in a real quantum dot. At half-filling, there is particle-hole symmetry where electrons (holes) can be exchanged via both the bare state at energy ϵ_0 and the one at $\epsilon_0 + U$. In this case, no shift of the Kondo peak is expected even if $\Gamma_s \neq \Gamma_d$. Extrapolating $G(T)$ to the unitary limit $G(0)$ at zero temperature (not shown) using the standard expression to fit the Kondo effect, i.e., $G(T) = G(0) / [1 + (2^{1/s} - 1) \times (T/T_K)^2]$,²⁹ we obtain for the ridge at charge state $N=3$ a zero temperature conductance of $G(0) = 1.68 e^2/h$, out of which the Γ ratio is estimated to be ≈ 2 . Hence, there is an asymmetry of magnitude comparable to Ref. 27. Our statement, that the shift of the Kondo peak to finite bias is absent

at half-filling, is beautifully reflected in the data of Fig. 5. Due to the fourfold symmetry, half-filling corresponds to charge state $N=2'$ and, indeed, this peak has its maximum at $V_{sd}=0$. The other two resonances are shifted oppositely, one to $V_{sd} > 0 (N=1')$ and the other to $V_{sd} < 0 (N=3')$. The shift amounts to 0.22 meV. These shifts are comparable in magnitude to the ones seen by Schimmel *et al.*, although they have observed only unipolar shifts. Finally, we remark that the transitions to the Coulomb blockade diamonds, i.e., $2' \leftrightarrow 1'$ and $3' \leftrightarrow 4'$, are asymmetric with respect to the V_{sd} (see arrows). Cross-sections at constant gate-voltage through these transitions allow us to deduce the respective Γ 's and their ratio: $\gamma := \Gamma_s/\Gamma_d$. We point out that this asymmetry is a consequence of the level degeneracy. Consider tunneling at finite bias into the $N=1'$ state. Because there is a fourfold degeneracy the effective in-tunneling rate is enhanced by a factor of 4. In contrast, this phase-space argument does not hold for the out-tunneling rate. The respective current steps are then given by $(4e/h)\Gamma_s\Gamma_d/(\Gamma_s+4\Gamma_d)$ for one bias polarity (e.g., $V_{sd} > 0$) and $(4e/h)\Gamma_s\Gamma_d/(4\Gamma_s+\Gamma_d)$ for the other polarity, where the factor 4 counts the degeneracy. It is clear from these two relations that the current steps are only different for the two polarities if $\gamma \neq 1$. The two current steps, measured for the transition $3' \leftrightarrow 4'$, amount to ≈ 20 and ≈ 30 nA, yielding for the Γ -ratio $\gamma \sim 2$ (in agreement to what we have deduced before in a different way) and $\Gamma_s \approx 1.4$ meV and $\Gamma_d \approx 0.7$ meV, so that the total level broadening is approximately $\Gamma \approx 2$ meV. Also the latter value is in agreement with the previously mentioned width of the transition, which we measured to be $\Gamma \approx 1.9$ meV.

After this extensive analysis we use the last part of this section to point to observed deviations. Figure 6 displays the dependance of the linear-response (a) and differential conductance (b) of another sample also contacted with Pd. The contact separation is longer and amounts to $L \sim 0.8 \mu\text{m}$. The linear-response conductance is bound by $2e^2/h$, suggesting that we measure through one individual SWNT. Fourfold clustering in the electron addition spectrum is observed for more than five shells ($A-E$), corresponding to 20 electrons. Due to the three times larger length of this device as compared to the one in Fig. 1 the energy scale is reduced by approximately a factor of 3. The level-spacing amounts to $\delta E \approx 1-1.5$ meV and the charging energy to $U \approx 1$ meV. The ratio $\delta E/U \approx 1$ as before. As with the data of Fig. 1 the Kondo effect may appear at half-filling (α) or may be absent (β), which according to the discussion above would correspond to the PE and S ground state, respectively. There are differences, however. The most dramatic one occurs in shell D for the three electron state (filling $\frac{3}{4}$), marked with O . Instead of the expected spin- $\frac{1}{2}$ Kondo, the conductance is actually suppressed. This is seen as a pronounced white bubble. Because the Kondo effect is present for the one electron state (filling $\frac{1}{4}$), this implies breaking of particle-hole symmetry. This effect is quite surprising and has not been reported before. We do not have a convincing explanation but mention one possibility. The three electrons at $N=3$ may like to form a high-spin state with total spin $S = \frac{3}{2}$. However, this requires three different orbitals, but there are only two in an ideal tube. It may be that the nanotube is not perfect,

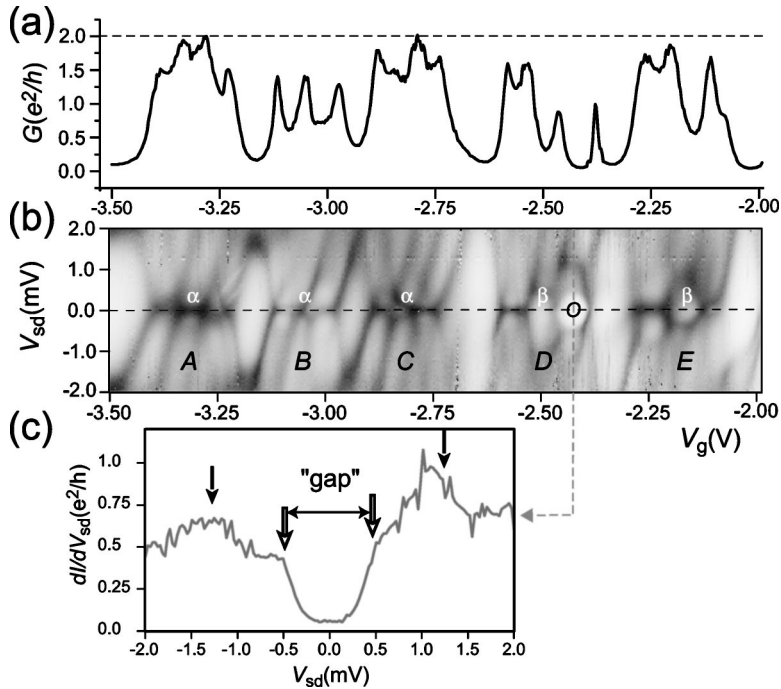


FIG. 6. (a) Linear response conductance plotted as a function of the gate voltage V_g and (b) differential conductance dI/dV_{sd} (darker more conductive) plotted as a function of V_g and V_{sd} for an another SWNT device with length $L \sim 800$ nm contacted by palladium. The shell pattern of four electrons each extends over five shells (A–E). The Kondo effect occurring at half-filling is marked with α , while β corresponds to the singlet ground state, and O points to an anomaly, a strong gap-feature arising for a three electron state. The nonlinear dI/dV_{sd} through the middle of this state is shown in (c).

rather a bundle or a multi-shell tube, which may provide additional orbitals. We think that this scenario is unlikely, because we just have shown that the exchange is small, and it is particularly small if the interaction is screened by other tubes. The gap may, however, be induced by a magnetic defect caused by residual catalyst particles, which may enhance the exchange energy. Due to the small size of catalyst particles such a defect interacts only locally. If efficient, one would expect a strong effect on the addition energy due to the large energy scale of the defect. In our opinion, the observed regularity of the addition pattern rules out disorder.

Similar gap-features are sometimes seen over the entire gray-scale plot. We show in Fig. 7 a short section taken out of an extensive differential conductance gray-scale plot of another sample. The contacting material is Au in this case and the contact separation amounts to $L \sim 1 \mu\text{m}$. The contact transparencies are lower here and typical two terminal conductances are of order $0.1 e^2/h$. Consequently, the main features in the differential-conductance are Coulomb blockade (CB) diamonds. The generic fourfold shell structure is not apparent. It is masked by the charging energy which dominates here. The observed addition energy amounts to ΔE

≈ 5 meV. We stress that the dI/dV_{sd} measurements of Fig. 7(a) extend over more than 17 electrons without any noticeably change. The linear-response conductance [Fig. 7(c)] shows a very regular set of high conductance peaks at the transition between neighboring charge states with peak values approaching $0.8 e^2/h$. The spacing between these CB-oscillation peaks is surprisingly constant, amounting to $\Delta V_g = 73 \pm 5$ mV. This yields a gate-coupling constant of $\alpha = 0.068$, which is comparable to the one deduced for the sample of Fig. 1 ($\alpha = 0.08$).

We present this measurement here, because of the presence of a striking gap-structure, which is seen inside of *all* CB diamonds and which might be related to the gap which we have mentioned before, i.e., the feature labelled O in Fig. 6(b). Two dI/dV_{sd} cross-sections at constant V_g are presented in Fig. 7(b). We find that the size of the gap Δ_g varies a bit in different charge state and is estimated to be $\Delta_g \approx 0.7$ meV (0.3, ..., 0.9 meV). Additional suppression may be caused, if the nanotube is split by a strong scattering center into two segments in series. In this case, however, a regular periodic CB-oscillation pattern is not expected, because single-electron transport requires that two charge states are degenerate.

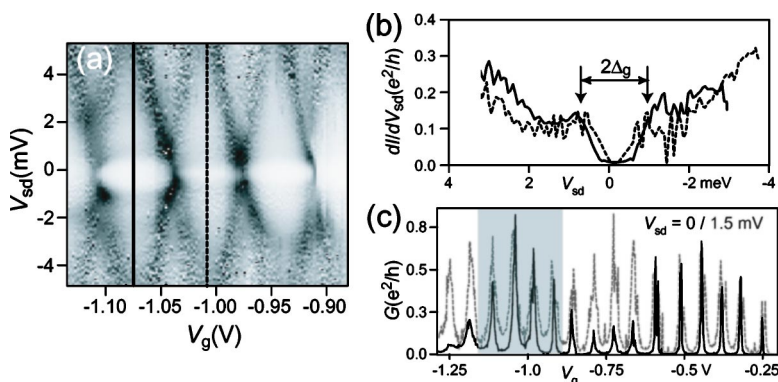


FIG. 7. (a) Differential-conductance plot of a SWNT device with contact separation $L \sim 1 \mu\text{m}$ at $T = 300$ mK (maximum conductance = e^2/h , black). Coulomb blockade diamonds are clearly seen. In addition gaps appear near zero bias. (b) dI/dV_{sd} as a function of V_{sd} and at constant V_g along the corresponding lines, shown in (a). Conductance as a function of gate voltage taken at $V_{sd} = 0$ (full) and $V_{sd} = 1.5$ mV (dashed). The shaded region corresponds to (a).

erate in both segments simultaneously. While this may be possible occasionally, it would be surprising if the levels would move in both segments with gate voltage exactly equally. We therefore are convinced that this scenario is wrong. Also a possible parallel conductance through two (or more) different tubes can be excluded, because this should appear in the gray-scale plot as a bare superposition of two CB patterns. Moreover, the observed gray-scale plot cannot be modeled as a regular CB pattern multiplied by a gap-feature in the vicinity of $V_{sd} \approx 0$. This is evident from the Fig. 7(c) which shows $G(V_g)$ at $V_{sd}=0$ (full curve) and at $V_{sd}=1.5$ mV (dashed curve). In the shaded region, corresponding to Fig. 7(a), the suppression is only active in between the CB-oscillation peaks, whereas the peaks themselves are not suppressed, suggesting that the $0d$ orbitals extend from source to drain. The low-conductance “bubbles” are therefore confined to the CB region of the nanotube and this new effect is observable in transport through a single carbon nanotube. This does not mean that there is only one single-walled carbon nanotube present. The device may still consist of a small bundle or a multishell tube, of which only one tube is effectively coupled to the reservoirs. In addition, the presence of magnetic impurities in the form of catalyst particles cannot be excluded, so that the observed gaps may originate from magnetic interactions with these particles. The Kondo effect which results in a high conductance resonance can be described as an anti-ferromagnetic exchange between

the leads and the quantum dot. It is tempting to suggest that the opposite scenario, namely ferromagnetic exchange with, for example, a magnetic particle, may suppress the conductance.³⁰

IV. CONCLUSION

In conclusion, we have analyzed the ground state of carbon nanotubes which are relatively strongly coupled to the attached leads. Spin- $\frac{1}{2}$ Kondo is present for charge states $N=1$ and $N=3$. At half-filling, i.e., for two electrons on the dot, the ground state is either a nondegenerate paired electron or a highly degenerate two-electron state. Whereas the Kondo effect is prohibited in the first case, it is allowed (and enhanced) in the second. The appearance of the Kondo effect at $N=2$ is largely determined by the magnitude of the level broadening Γ , caused by the coupling to the leads. We have also observed striking gaps whose origin need to be unravelled in the future.

ACKNOWLEDGMENTS

We acknowledge contributions and discussions to this work by W. Belzig, V. N. Golovach, D. Loss, and L. Forró (EPFL). Support by the Swiss National Science Foundation, the NCCR on Nanoscience and the BBW (Cost and RTN DIENOW) is gratefully acknowledged.

*Electronic address: christian.schoenenberger@unibas.ch; URL: www.unibas.ch/phys-meso

¹See, e.g., M. S. Dresselhaus, G. Dresselhaus, and P. C. Eklund, *Science of Fullerenes and Carbon Nanotubes* (Academic, New York, 1996).

²C. Dekker, *Phys. Today* **52**(5), 22–28 (1999).

³S. J. Tans, R. M. Verschueren, and C. Dekker, *Nature (London)* **394**, 761 (1998).

⁴H. Grabert and M. H. Devoret, *Single Charge Tunneling, Coulomb Blockade Phenomena in Nanostructures* (Plenum, New York, 1992); L. P. Kouwenhoven, C. M. Marcus, P. L. McEuen, S. Tarucha, R. M. Westervelt, and N. S. Wingreen, “Electron transport in quantum dots,” in *Proceedings of the NATO Advanced Study Institute on Mesoscopic Electron Transport* (Series E345), (Kluwer, Dordrecht, 1997).

⁵D. Goldhaber-Gordon, H. Shtrikman, D. Mahalu, D. Abusch-Magder, U. Meirav, and M. A. Kastner, *Nature (London)* **391**, 156 (1998).

⁶L. Kouwenhoven and L. Glazman, *Phys. World* **14**, 33 (2001).

⁷W. Liang, M. Bockrath, D. Bozovic, J. H. Hafner, M. Tinkham, and H. Park, *Nature (London)* **411**, 665 (2001).

⁸J. Nygård, D. Cobden, and P. E. Lindelof, *Nature (London)* **408**, 342 (2000).

⁹W. D. Knight, C. Klemenger, W. A. de Heer, W. A. Saunders, M. Y. Chou, and M. L. Cohen, *Phys. Rev. Lett.* **52**, 2141 (1984).

¹⁰S. Tarucha, D. G. Austing, T. Honda, R. J. van der Hage, and L. P. Kouwenhoven, *Phys. Rev. Lett.* **77**, 3613 (1996).

¹¹M. R. Buitelaar, A. Bachtold, T. Nussbaumer, M. Iqbal, and C.

Schönenberger, *Phys. Rev. Lett.* **88**, 156801 (2002).

¹²J. Kong, A. M. Cassel, and H. Dai, *Chem. Phys. Lett.* **292**, 567–574 (1998); J. H. Hafner, M. J. Bronikowski, B. R. Azamian, P. Nikolaev, A. G. Rinzler, D. T. Colbert, K. A. Smith, and R. E. Smalley, *ibid.* **296**, 195–202 (1998); J. Kong, H. T. Soh, A. M. Cassel, C. F. Quate, and H. Dai, *Nature (London)* **395**, 878–881 (1998).

¹³W. Liang, M. Bockrath, and H. Park, *Phys. Rev. Lett.* **88**, 126801 (2002).

¹⁴B. Babić, J. Fuhrer, M. Iqbal, and C. Schönenberger, in *Electronic Properties of Synthetic Nanostructures*, edited by H. Kuzmany, J. Fink, M. Mehring, and S. Roth (AIP, New York, 2004), AIP Conf. Proc. **723**, 574 (2004).

¹⁵B. Babić, M. Iqbal, and C. Schönenberger, *Nanotechnology* **14**, 327 (2003).

¹⁶A. Javey, J. Guo, Q. Wang, M. Lundstrom, and H. Dai, *Nature (London)* **424**, 654 (2003).

¹⁷Y. Meir, N. S. Wingreen, and P. A. Lee, *Phys. Rev. Lett.* **70**, 2601 (1993).

¹⁸Y. Oreg, K. Byczuk, and B. I. Halperin, *Phys. Rev. Lett.* **85**, 365 (2000).

¹⁹D. V. Averin, A. N. Korotkov, and K. K. Likharev, *Phys. Rev. B* **44**, 6199 (1991); C. W. Beenaker, *ibid.* **44**, 1646 (1991).

²⁰S. Sasaki, S. De. Franceschi, J. M. Elzerman, W. G. van der Wiel, M. Eto, S. Tarucha, and L. P. Kouwenhoven, *Nature (London)* **405**, 764 (2000).

²¹M. Eto and Y. V. Nazarov, *Phys. Rev. Lett.* **85**, 1306 (2000).

²²A. Fuhrer, T. Ihn, K. Ensslin, W. Wegscheider, and M. Bichler,

- Phys. Rev. Lett. **91**, 206802 (2003).
- ²³M. Pustilnik and L. Glazman, Phys. Rev. Lett. **85**, 2993 (2000).
- ²⁴M. Pustilnik, L. Glazman, D. H. Cobden, and L. P. Kouwenhoven, Lect. Notes Phys. **579**, 3 (2001).
- ²⁵M. Pustilnik, L. Borda, L. I. Glazman, and J. von Delft, cond-mat/0309646.
- ²⁶D. H. Cobden, M. Bockrath, P. L. McEuen, A. G. Rinzler, and R. E. Smalley, Phys. Rev. Lett. **81**, 681 (1998).
- ²⁷F. Simmel, R. H. Blick, J. P. Kotthaus, W. Wegscheider, and M. Bichler, Phys. Rev. Lett. **83**, 804 (1999).
- ²⁸M. Krawiec and K. I. Wysokiński, Phys. Rev. B **66**, 165408 (2002).
- ²⁹T. A. Costi, A. C. Hewson, and V. Zlatic, J. Phys.: Condens. Matter **6**, 2519 (1994).
- ³⁰G. A. Fiete, G. Zarand, and B. I. Halperin, Phys. Rev. B **66**, 024431 (2002).